Electronic Specific Heat of Iron Pnictides Based on Electron-Cooper Pair Interaction

Abel Mukubwa

Department of Science, Technology and Engineering, Faculty of Science, Kibabii University, Bungoma, Kenya
Email: abelmuwa@gmail.com

Abstract

The discovery of iron pnictides in 2006 added on the number of materials that have the potential to transmit electricity with close zero d.c resistance. High-temperature iron-based superconductors have been obtained through modification, mostly by doping, of the initially low-temperature iron-based superconductors. Unlike in LTSC, the energy gap in HTSC requires a theory, beyond spin fluctuations, to explain its anisotropy. This study seeks to establish a common ground between iron pnictides and cuprates towards explaining high temperature superconductivity. There is a general consensus on the existence of Cooper pairs in these systems. In addition to this, experimental results have revealed the existence of electron-boson coupling in iron pnictides. These results make it viable to study the interaction between an electron and a Cooper pair in iron based superconductors (IBSC). In this study, Bogoliubov-Valatini transformation has been used in determining the electronic specific heat based on the interaction between an electron and a Cooper pair in high-temperature IBSC, namely, $Ca_{0.33}Na_{0.6}Fe_2As_2$ and $SmFeAsO_{0.8}F_{0.2}$. We record the theoretical electronic specific heat of $CeFeAsO_{0.84}F_{0.16}$ and $SmFeAsO_{0.8}F_{0.2}$ as 164.3 mJ mol^{-1} K^{-2} and 101.6 mJ mol^{-1} K^{-2} respectively.

Subject Areas

Chemical Engineering & Technology

Keywords

Superconductivity, Iron Pnictides, Specific Heat Capacity

1. Introduction

The discovery of superconductivity by Onnes (1911) raised many questions about the properties of superconducting materials. It was not until 1933, that the

interaction between superconductors and magnetic fields was brought to limelight [1]. The magnetic field around a superconductor is related to the current flowing (that results to electric field) through a superconductor by the London equations [2]. The penetration depth into a superconductor and the magnetic fields around the superconductor are related by the Ginzburg-Landau equations [3]. Later on, it was established that superconductivity is hinged on the pairing of electrons at the Fermi surface that lead to the formation of Cooper pairs [4]. The microscopic theory of superconductivity, based on s-wave pairing, laid the general foundation not only for conventional superconductivity, but also for unconventional superconductivity. However, in conventional superconductivity, the Cooper pair is not considered in isolation as is the case with conventional superconductivity [5] [6]. Furthermore, the challenge in high temperature superconductivity (HTS) is that the manner in which the electron-boson interaction occurs is still unknown [6]. Thus, the pairing mechanism in high temperature superconductors below the critical temperature remains unclear.

Secondly, the size of the energy gap is an important factor that contributes towards the superconductivity of a material. In general, the critical temperature of a material increases with the energy gap of the material. In HTSC, many theoretical formulations linking the energy gap to the critical temperature of a HTSC material have been developed, but they do not replicate [7]. The energy gap in HTS is anisotropic along the Fermi surface, unlike that in low temperature superconductors (LTSC) [8].

HTSC was born with the discovery of a Lanthanum-based cuprate [9]. A yttrium-based cuprate was discovered a year later when lanthanum was replaced with yttrium $LBCuO_4$ [10]. The highest critical temperature so far reached at ambient pressure 138 K in mercury based cuprate and 203 K in Sulphur hydride, under extremely high pressure of about 200 GPa [11] [12]. Cuprates have been the only known group of high temperature until 2006 when properties of superconductivity were observed in a lanthanum based iron pnictide [13]. Following this discovery, other iron-based superconductors have since been discovered. Iron-based conductors are generally classified as 11 (e.g. FeSe), 111 (e.g. LiFeAs), 122 (e.g. $LaFe_2As_{1-x}P_x$), and 1111 (e.g. $BaFeAsO_{1-x}F_x$) [14]. **Figure 1** below shows the structure of 1111-type (a), 122-type (b), 1111 (c) and 11-type (d).

Though FeAs appears in the 111-, 122- and 1111-type, the layers that separate FeAs vary from one type to another. However, Fe is blocked immediately from both sides in all the four categories. Of interest among the four families is the 1111-type, because the high critical temperatures for these materials have been recorded.

Electron-phonon interactions and spin fluctuations are central to the mechanism of HTS [15]. It has been widely agreed upon that superconductivity in cuprates results from electron-phonon interactions that form Cooper pairs. On the other hand, superconductivity in IBSC has been attributed to spin fluctuations. Spin fluctuations have sufficient strength to mediate the pairing interactions in high-temperature superconductivity except that the estimates of the
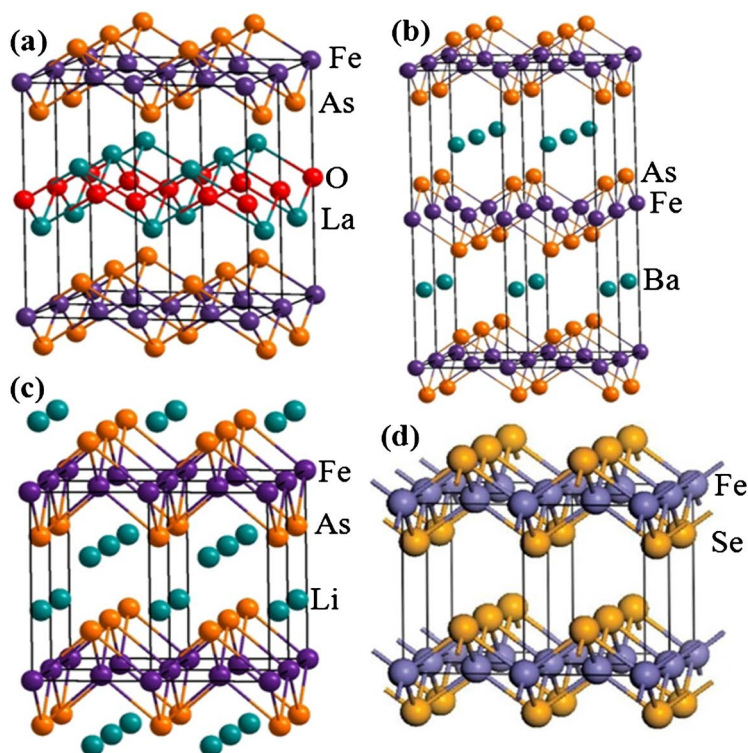
Figure 1. Four families of iron-based superconductors, (a) 1111, (b) 122, (c) 111, (d) 11 type. Adapted from Hyungju *et al.*, 2011.

strengths of this interaction differ widely [16]. HTS requires a theory, beyond spin fluctuations, to explain the anisotropic nature of its energy gap [17]. Spin fluctuations is a convenient way to describe multiple Coulomb interactions between fermions [18]. IBSCs can be treated as moderately interacting itinerant fermionic systems with multiple FS sheets and effective four-fermion intra-band and inter-band interactions in the band basis [18]. There is general consensus on the unconventional nature of the Cooper pairing state of IBSC in multiple energy gaps and Fermi surfaces [19]. Based on this understanding, the origin of Cooper pairing in IBSC ($Ba_{1-x}K_xFe_2As_2$) has been studied using Raman spectroscopy to probe the structure of the pairing interaction at play in the superconductor [20]. The spectra collected in the B_{1g} symmetry channel reveal the existence of two collective modes which are indicative of the presence of two competing pairing tendencies of $d_{x^2-y^2}$ symmetry type. Bohm *et al.* (2018) has considered this pairing as the basis of the formation of Cooper pairs in the IBSC. The d-wave gap in IBSCs has dependence on the electron Fermi surfaces and may be nodeless in some cases [21]. Other than electrons pairing, interactions between electrons and bosons have also been observed in IBSC.

Experimental results based on time-resolved spectroscopy have also shown that there exists electron-boson coupling in IBSC [22] [23]. While cuprates show a single energy gap with one Fermi surface (FS), a point-contact Andreev-reflection study of $Ba(Fe_{1-x}Co_x)_2As_2$ single crystals has revealed that there exists a multigap band and multiple Fermi surfaces with a four-fermion intraband and interband

interactions in the band basis [23]. Because the Fermi level of each parent compound is primarily governed by the five 3d orbitals of iron ion, iron plays a primary role in the superconductivity [21]. In most cases, removing the magnetism is an experimental step needed for the emergence of superconductivity. For the 1111 system, T_c appears when the antiferromagnetism (AFM) disappears but the AFM and superconductivity coexist in the 122 system [21]. The energy gaps in HTS are largely anisotropic. It has been argued that the electron correlation effect should be considered to explain the anisotropic transport properties of the general d/f valence electron system [17] [24]. Based on these findings, I argue that interaction between electrons and Cooper pairs may as well be used to study the thermodynamic properties of IBSC just as it has been the case for cuprates. The Cooper pair in this interaction plays the part of a boson [25]. The IBSC materials to be considered under this study are $CeFeAsO_{0.84}F_{0.16}$ with a T_c of 34 K while $SmFeAsO_{0.8}F_{0.2}$ with $T_c = 54$ K.

High temperature superconductors have a vast applications some of which include maglev trains, Superconducting Quantum Interface Devices (SQUIDs) and Magnetic Resonance Imaging (MRI). Understanding the pairing mechanism in HTSC superconductors will enhance theoretical predictions, with precision, of the T_C's as well as other thermodynamic properties of high temperature superconductors [26]. This will open avenues to discoveries towards room-temperature superconductivity (RTS). Though the number of High temperature iron-based high temperature superconductors is on increase, theoretical as well as experimental studies are still conflicting with the observed properties [7] [27] [28].

Superconductivity majorly results from the formation of Cooper pairs, at the Fermi surface, at the critical temperature. However, not all electrons at the Fermi surface take part in the formation of Cooper pairs, giving rise to a phenomenon in which Cooper pairs interact with the free electrons. This model has been used to study cuprates and the resulting entropy and specific heat showed close proximity to the results from previously done experimental and theoretical work [7] [26]. However, the energy due to electron interaction is found to be much less than the measured energy gap in cuprates. The difference arises from the fact that the measured energy gap represents the energy due to both electron-electron interaction and electron-phonon interactions [7]. The BVT has previously yielded results that are in agreement with other methods such as second quantization [26]. In this approach, a Hamiltonian of interaction between the electron and the Cooper pair is first developed using the kinetic energies of both the electron and the Cooper pair, the positive interaction potential and the negative interaction potential. Row reducing the Hamiltonian leads to energy of the system at condensate state. The specific heat of the system has been deduced from the expression of the system's energy.

2. Theoretical Framework

To start with, the Cooper pair and the electron are considered to occupy differ-

ent states. The total Hamiltonian, for the interaction is given by

$$H = H_0 + H_P \tag{1}$$

where, H_0 is the Hamiltonian of interaction between a Cooper pair in state k and electron in state q for unperturbed system and is given by

$$H_0 = \sum_q \epsilon_q a_q^\dagger a_q + \sum_k \epsilon_k b_k^\dagger b_k \tag{2}$$

H_P is the Hamiltonian for the perturbed system and is given by

$$H_P = \sum_{k,q} V_{k,q} a_q^\dagger a_q \left(b_k^\dagger - b_k \right) - \sum_{q,k} U_k a_q^\dagger a_q b_k^\dagger b_k \tag{3}$$

From Equations (2) and (3), $a_q^\dagger (a_q)$ is the creation (annihilation) operator for an electron in state q, $b_k^\dagger = a_k^\dagger a_{-k}^\dagger$ ($b_k = a_{-k} a_k$) is the creation (annihilation) operator for the Cooper pair in state k; $a_q^\dagger a_q$ and $b_k^\dagger b_k$ are the number operators for an electron and a Cooper pair respectively, $\epsilon_q = \hbar k_e^2 / 2m_e$ is the kinetic energy for electron and $\epsilon_k = \hbar k_c^2 / 2m_c$ is the kinetic energy for the Cooper pair.

Equations (2) and (3), when combined, give the Hamiltonian for a perturbed system as

$$H = \sum_q \epsilon_q a_q^\dagger a_q + \sum_k \epsilon_k b_k^\dagger b_k + \sum_{k,q} V_{k,q} a_q^\dagger a_q \left(b_k^\dagger - b_k \right) - \sum_{k,q} U_k a_q^\dagger a_q b_k^\dagger b_k \tag{4}$$

Equation (3) is then written in terms of Bogoliubov-Valatini operators, γ, using the relations $a_k = u_q \gamma_q + v_q \gamma_{-q}^+$, $a_{-k} = u_k \gamma_{-k} - v_k \gamma_k^+$, $a_k^\dagger = u_q \gamma_q^+ + v_q \gamma_{-q}$ and $a_{-k}^\dagger = u_k \gamma_{-k}^+ - v_k \gamma_k$. Where, $|u_k|^2$ is the probability that the pair state {$k,-k$} within a certain interval around the Fermi level is unoccupied and $|v_k|^2$ is the probability that the pair state {$k,-k$} within a certain interval around the Fermi level is occupied (k is a wave vector). Thus,

$$
\begin{aligned}
H = &\sum_q \epsilon_q \left\{ u_q^2 m_q + v_q^2 \left(1 - m_{-q} \right) + u_q v_q \left(\gamma_q^+ \gamma_{-q}^+ + \gamma_{-q} \gamma_q \right) \right\} \\
&+ \sum_k \epsilon_k \left\{ u_k^4 m_{-k} m_k - u_k^2 v_k^2 m_k \left(1 - m_{-k} \right) + u_k^2 v_k^2 \left(1 - m_k \right) m_k \right. \\
&+ u_k^2 v_k^2 \left(1 - m_{-k} \right) m_{-k} - u_k^2 v_k^2 \left(1 - m_{-k} \right) m_k + v_k^4 \left(1 - m_{-k} \right) \left(1 - m_k \right) \\
&\left. + \left\{ u_k^3 v_k \left(m_{-k} + m_k \right) + v_k^3 u_k \left(2 - m_k - m_{-k} \right) \right\} \left(\gamma_k^+ \gamma_{-k}^+ + \gamma_{-k} \gamma_k \right) \right\} \\
&+ \sum_{k,q} V_{k,q} \left\{ \left\{ u_q^2 m_q + v_q^2 \left(1 - m_{-q} \right) \right\} \left(\gamma_k^+ \gamma_{-k}^+ - \gamma_{-k} \gamma_k \right) \right\} \\
&- \sum_{k,q} U_k \left\{ u_k^4 u_q^2 m_{-k} m_k m_q + u_k^4 v_q^2 m_k \left(1 - m_{-q} \right) m_{-k} \right. \\
&+ u_q^2 v_k^4 \left(1 - m_k \right) \left(1 - m_{-k} \right) m_q + v_q^2 v_k^4 \left(1 - m_{-k} \right) \left(1 - m_{-q} \right) \left(1 - m_k \right) \\
&+ u_q^2 u_k^2 v_k^2 m_q \left[m_k \left(1 - m_k \right) - 2 m_k \left(1 - m_{-k} \right) + m_{-k} \left(1 - m_{-k} \right) \right] \\
&+ u_k^2 v_k^2 v_q^2 \left(1 - m_{-q} \right) \left[\left(1 - m_k \right) m_k - 2 \left(1 - m_{-k} \right) m_k + \left(1 - m_{-k} \right) m_{-k} \right] \\
&+ \left[u_k^3 u_q^2 v_k \left(m_{-k} + m_k \right) m_q + u_k^3 v_q^2 v_k \left(m_{-k} + m_k \right) \left(1 - m_{-q} \right) \right. \\
&\left. + v_k^3 u_q^2 u_k \left(2 - m_k - m_{-k} \right) m_q + v_k^3 v_q^2 u_k \left(1 - m_{-q} \right) \left(2 - m_k - m_{-k} \right) \right] \\
&\times \left(\gamma_k^+ \gamma_{-k}^+ + \gamma_{-k} \gamma_k \right) + \left[u_k^2 v_k^2 u_q v_q \left(1 - m_{-k} \right) m_{-k} - 2 u_k^2 v_k^2 u_q v_q m_k \left(1 - m_{-k} \right) \right. \\
&\left. + u_k^2 v_k^2 u_q v_q \left(1 - m_k \right) m_k + u_k^4 u_q v_q m_{-k} m_k + v_k^4 u_q v_q \left(1 - m_{-k} \right) \left(1 - m_k \right) \right] \\
&\left. \times \left(\gamma_q^+ \gamma_{-q}^+ + \gamma_{-q} \gamma_q \right) \right\} + 4OT
\end{aligned}
\tag{5}
$$

where 4OT are the fourth order terms.

1) Energy of the System

The diagonal part of the effective Hamiltonian represents the energy of the system when it is in equilibrium. Therefore, at equilibrium the energy of the system is then given by

$$
\begin{aligned}
E_k = &\sum_q \epsilon_q \left\{ u_q^2 m_q + v_q^2 \left(1 - m_{-q}\right) \right\} + \sum_k \epsilon_k \left\{ u_k^4 m_{-k} m_k - u_k^2 v_k^2 m_k \left(1 - m_{-k}\right) \right. \\
&+ u_k^2 v_k^2 \left(1 - m_k\right) m_k + u_k^2 v_k^2 \left(1 - m_{-k}\right) m_{-k} - u_k^2 v_k^2 \left(1 - m_{-k}\right) m_k \\
&\left. + v_k^4 \left(1 - m_{-k}\right)\left(1 - m_k\right) \right\} - \sum_{k,q} U_{k,q} \left\{ u_k^4 u_q^2 m_{-k} m_k m_q + u_k^4 v_q^2 m_k \left(1 - m_{-q}\right) m_{-k} \right. \\
&+ u_q^2 v_k^4 \left(1 - m_k\right)\left(1 - m_{-k}\right) m_q + v_q^2 v_k^4 \left(1 - m_{-k}\right)\left(1 - m_{-q}\right)\left(1 - m_k\right) \\
&+ u_q^2 u_k^2 v_k^2 m_q \left[m_k \left(1 - m_k\right) - 2 m_k \left(1 - m_{-k}\right) + m_{-k} \left(1 - m_{-k}\right) \right] \\
&\left. + u_k^2 v_k^2 v_q^2 \left(1 - m_{-q}\right) \left[\left(1 - m_k\right) m_k - 2 \left(1 - m_{-k}\right) m_k + \left(1 - m_{-k}\right) m_{-k} \right] \right\}
\end{aligned}
\tag{6}
$$

At equilibrium, the quasi-particles represented by the operators γ's are very few or do not exist and therefore, $m_k = m_{-k} = 0$ and $m_q = m_{-q} = 0$. Thus, Equation (6) becomes

$$
E_k = \sum_q \epsilon_q v_q^2 + \epsilon_k v_k^4 - v_k^4 \sum_q U_{k,q} v_q^2
\tag{7}
$$

For the electron to interact with the Cooper pair, they must be in the same state *i.e.* at the time of interaction we only consider the state k of the electron and neglect all the other states in q and therefore Equation (6) becomes,

$$
E_k = \epsilon_q v_k^2 + \epsilon_k v_k^4 - v_k^4 U_{k,k} v_k^2
\tag{8}
$$

For the three electron interaction to take place, the cooper pair and the electron involved in the interaction must be present. Thus, $v_k = 1$ and $u_k = 1$,

$$
E_k = \epsilon_q + \epsilon_k - U_{k,k}
\tag{9}
$$

To introduce temperature dependence, the energy E_k is multiplied by the thermal activation factor $\exp\left(\dfrac{-E_k}{K_B T}\right)$ where E_k is energy of the system and K_B is the Boltzmann constant. This produces a temperature dependent energy E_T given as

$$
E_T = E_k \mathrm{e}^{\left(\frac{-E_k}{K_B T}\right)}
\tag{10}
$$

2) Electronic Specific Heat Capacity

In finding the electronic specific heat, we first use the specific heat capacity of the system. The specific heat is expressed, as a function of the total energy of the system, using the expression

$$
C_v = \frac{\partial E_T}{\partial T}
\tag{11}
$$

For the three-electron system, we substitute (11) into (10) so that,

$$
C_v = \left[\frac{E_k^2}{K_B T^2} \right] \mathrm{e}^{\left(\frac{-E_k}{K_B T}\right)}
\tag{12}
$$

The Sommerfeld's coefficient is determined from the specific heat as

$$\gamma = \frac{C_v}{T} \tag{13}$$

Substituting (12) into (13)

$$\gamma = \left[\frac{E_k^2}{K_B T^3}\right] e^{\left(\frac{-E_k}{K_B T}\right)} = \left[\frac{4K_B T^2}{T^3}\right] e^{\left(\frac{-2T_c}{T}\right)} \tag{14}$$

3. Results and Discussion

The total energy of a system results from the interaction between the particles of the system. The energy due to interaction between these particles increases with the temperature of the system. At the temperature $T = T_c$, the material changes from a superconducting to a normal state. Figure 2 shows the total energy of electron-Cooper pair interaction in of Y123 as a function of temperature.

This half-stretched sigmoid curve has been obtained previously by other researchers when they were relating energy of the system to temperature [29]. From the graph, it is observed that the energy of the system increases with temperature but not linearly. In determining the critical point on the curve, the line $x = T_c$ has been used, that is, $x = 34$ for $Ca_{0.32}Na_{0.68}Fe_2As_2$ and $x = 55$ for $SmFeAsO_{0.8}F_{0.2}$. The energy of interaction between an electron and a Cooper pair at the critical temperature in $SmFeAsO_{0.8}F_{0.2}$ at is 1.26 meV, while that in $Ca_{0.32}Na_{0.68}Fe_2As_2$ is 0.6 meV. Comparatively, the energy of the three-electron model in thallium based cuprates, Tl2201, Tl2212 and Tl2223 were determined as 2.2 meV, 2.5 meV, and 2.9 meV while that of YBCO123 is found to be 2.2
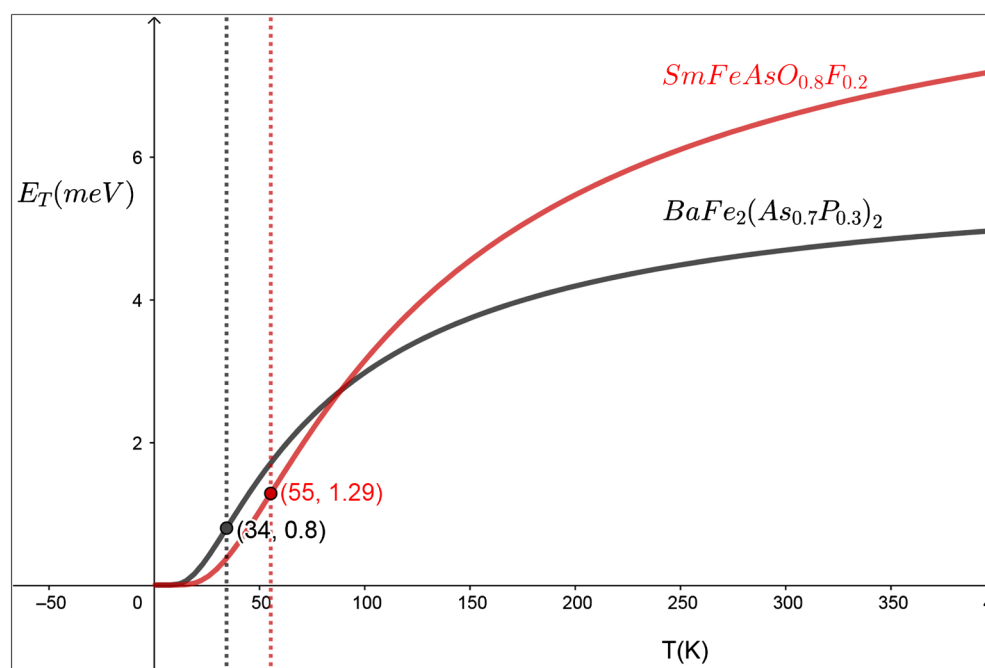

Figure 2. Energy of interaction between an electron and a Cooper pair in $SmFeAsO_{0.8}F_{0.2}$ and $Ca_{0.32}Na_{0.68}Fe_2As_2$ as a function of temperature.

meV [26] against the experimental 34 meV [5]. These energies are very low compared to the experimental energy values.

Electronic Specific Heat Capacity (γ)

Figure 3 represents graph of the electronic specific heat as a function of temperature for the two IBSCs under study.

Similar results were obtained by other researchers while comparing the variations in the electronic specific heat with temperature in cuprates [7] [26]. From Figure 3, the electronic specific heat for $CeFeAsO_{0.84}F_{0.16}$ and $SmFeAsO_{0.8}F_{0.2}$ are found to be 164.3 mJmol^{-1}K^{-2} and 101.6 mJmol^{-1}K^{-2} respectively. The electronic specific heat of $CeFeAsO_{0.84}F_{0.16}$ has been determined by measurement as 105 ± 5 mJmol^{-1}K^{-2} [30]. The theoretical value is of the same order as the experimental value. The method used in this work has been found to agree with the highest measured value for electronic specific heat of a Yttrium based cuprate, YBCO123 with γ = 60 mJmol^{-1}K^{-2} [26] [31].

The difference in the electronic specific heat between the theoretical value and the measured value may arise due to the quality of the sample used in the experimental approach [30]. For instance, working on the quality of $Ca_{0.33}Na_{0.67}Fe_2As_2$ to $Ca_{0.32}Na_{0.68}Fe_2As_2$ improves its electronic specific heat from 39 mJmol^{-1}K^{-2} to 105 mJmol^{-1}K^{-2}. Therefore, working on the quality of the substance can improve the measured values significantly and is likely to agree with the theoretical values obtained using this approach.

4. Conclusion

For the first time, the specific heat of iron pnictides has been determined based on a theoretical approach. The interaction between an electron and a Cooper
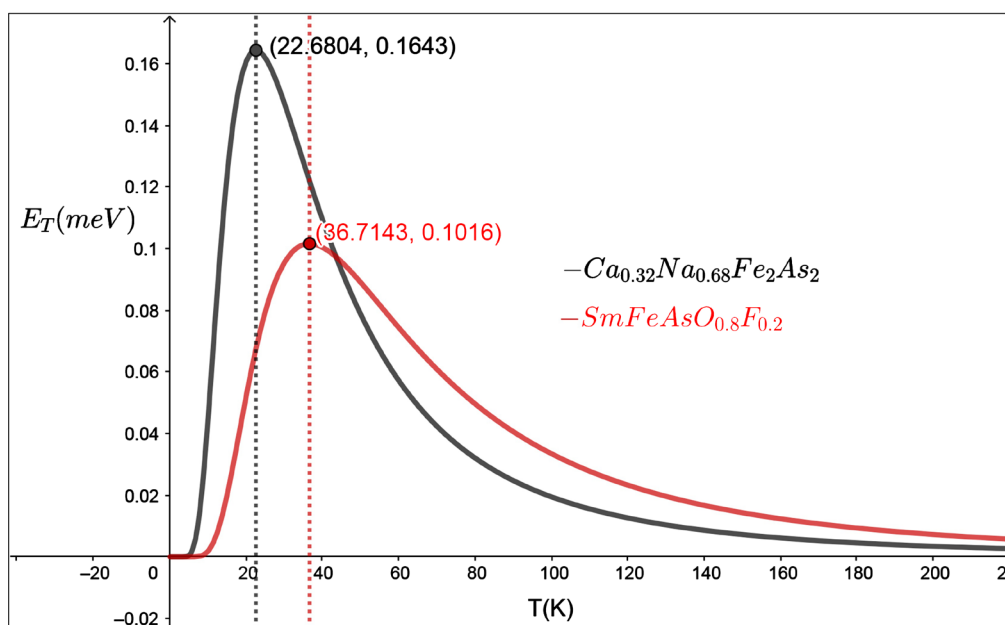

Figure 3. Graph of electronic of specific heat of $Ca_{0.32}Na_{0.68}Fe_2As_2$ and $SmFeAsO_{0.8}F_{0.2}$ as a function of temperature.

pair has successfully given values that are in close proximity to the measured values of the specific heat. Despite the differences in the origin of Cooper pairing, the electronic specific heats in both high temperature IBSC and cuprates depend on the electron-Cooper pair interaction. However, the energy obtained using this approach varies significantly from the experimental results confirming that electron-Cooper pair interaction and even spin fluctuations are not sufficient to explain HTSC. These findings reveal that the mechanism behind HTSC in both cuprates and IBSC is likely to be the same though the origin of pairing may vary.

Conflicts of Interest

The author declares no conflicts of interest regarding the publication of this paper.

References

[1] Meissner, W. and Ochsenfeld, R. (1933). Ein Neuer Effekt bei Eintritt der Supraleitfahigkeit. *Naturwissenschaften*, **21**, 787-788. https://doi.org/10.1007/BF01504252

[2] London, F. and London, H. (1935) The Electromagnetic Equations of the Supraconductor. *Proceedings of the Royal Society A*, **149**, 71-88. https://doi.org/10.1098/rspa.1935.0048

[3] Ginzburg, V.L. and Landau, L.D. (1950) On the Theory of Superconductivity. *Sov. Phys. JETP*, **20**, 1064.

[4] Bardeen, J., Cooper, L.N. and Schrieffer, J.R. (1957) The Microscopic Theory of Superconductivity. *Physics Review*, **108**, 1175. https://doi.org/10.1103/PhysRev.108.1175

[5] Nakayama, K., Sato, T., Terashima, K., Matsu, H., Takahash, T., Kubota, M., Ono, K., Nishizaki, T., Takahashi, Y. and Kobayashi, N. (2007) Bulk and Surface Low-Energy Excitations in $YBa_2Cu_3O_{7-\delta}$ Studied by High-Resolution Angle-Resolved Photoemission Spectroscopy. *Physical Review B*, **75**, Article ID: 014513. https://doi.org/10.1103/PhysRevB.75.014513

[6] Iwasawa, H., Yoshida, Y., Hase, I., Shimada, K., Namatame, H., Taniguchi, M. and Aiura, Y. (2013) "True" Bosonic Coupling Strength in Strongly Correlated Superconductors. *Scientific Report*, **3**, 1-4. https://doi.org/10.1038/srep01930

[7] Odhiambo, J.O. and Makokha, J.W. (2018) Specific Heat and Entropy of a Three Electron Model in Bismuth Based Cuprate Superconductor. *World Journal of Applied Physics*, **3**, 19-24.

[8] Tsuei, C. and Kirtley, R. (2002) D-Wave Pairing Symmetry in Cuprate Superconductors—Fundamental Implications and Potential Applications. *Physica C: Superconductivity*, **367**, 1-8. https://doi.org/10.1016/S0921-4534(01)00976-5

[9] Bednorz, G.J. and Muller, K.A. (1986) Possible High TC Superconductivity in the La-Ba-Cu-O System. *Zeitschrift für Physik B Condensed Matter*, **64**, 189-193. https://doi.org/10.1007/BF01303701

[10] Wu, M.K., Ashburn, J.R., Torng, C.J., Hor, P.H., Meng, R.L., Gao, L., Huang, Z.J., Wang, Y.Q. and Chu, C.W. (1987) Superconductivity at 93 K in a New Mixed-Phase Y-Ba-Cu-O Compound System at Ambient Pressure. *Physical Review Letters*, **58**, 908. https://doi.org/10.1103/PhysRevLett.58.908

[11] Onbasli, U., Wang, Y.T., Naziripour, A., Tello, R., Kiehl, W. and Hermann, A.M. (1996) Transport Properties of High-TC Mercury Cuprates. *Physica Status Solidi* (*b*), **194**, 371-382. https://doi.org/10.1002/pssb.2221940131

[12] Drozdov, A.P., Eremets, M.I., Troyan, I.A., Ksenofontov, V. and Shylin, S.I. (2015) Conventional Superconductivity at 203 Kelvin at High Pressures in the Sulfur Hydride System. *Nature*, **525**, 73-76. https://doi.org/10.1038/nature14964

[13] Kamihara, Y., Hiramatsu, H., Hirano, M., Kawamura, R., Yanagi, H., Kamiya, T. and Hosono, H. (2006) Iron-Based Layered Superconductor: LaOFeP. *Journal of the American Chemical Society*, **128**, 10012-10013. https://doi.org/10.1021/ja063355c

[14] Oh, H., Moon, J., Shin, D., Moon, C.-Y. and Choi, H.J. (2011) Brief Review on Iron-Based Superconductors: Are There Clues for Unconventional Superconductivity? *Progress in Superconductivity*, **13**, 65-84.

[15] Malik, M.A. and Malik, B.A. (2014) High Temperature Superconductivity: Materials, Mechanisms and Applications. *Bulgarian Journal of Physics*, **41**, 305-314.

[16] Dahm, T., Hinkov, V., Borisenko, V., Kordyuk, A.A., Zabolotny, V.B., Fink, J., Buchner, B., Scalapino, D.J., Hanke, W. and Keimer, B. (2009) Strength of the Spin-Fluctuation-Mediated Pairing Interaction in High-Temperature Superconductor. *Nature Physics*, **5**, 217-221.

[17] Yoshida, T., Ideta, S., Shimojima, T., Malaeb, W., Shinada, K., Suzuki, H., Nishi, I., Fujimori, A., Ishizaka, K., Shin, S., Nakashima, Y., Anzai, H., Arita, M., Ino, A., Namatame, H., Taniguchi, M., Kumigashira, H., Ono, K., Kasahara, S., Shibauchi, T., Terashima, T., Matsuda, Y., Nakajima, M., Uchida, S., Tomioka, Y., Ito, T., Kihou, K., Lee, C.H., Iyo, A., Eisaki, H., Ikeda, H., Arita, R, Saito, T., Onari, S. and Kontani, H. (2014) Anisotropy of the Superconducting Gap in the Iron-Based Superconductor $BaFe_2(As_{1-x}P_x)_2$. *Scientific Report*, **4**, 7292. https://doi.org/10.1038/srep07292

[18] Chubukov, A.V., Efremov, D.V. and Eremin, I. (2008) Magnetism, Superconductivity and Pairing Symmetry in Iron-Based Superconductors. *Physics Review B*, **78**, Article ID: 134512. https://doi.org/10.1103/PhysRevB.78.134512

[19] Paglione, J. and Greene, R. (2018) High-Temperature Superconductivity in Iron-Based Materials. https://doi.org/10.1038/nphys1759

[20] Böhm, T., Kretzschmar, F., Baum, A., Rehm, M., Jost, D., Ahangharnejhad, R.H., Thomale, T., Platt, C., Maier, T.A., Hanke, W., Moritz, B., Devereaux, T.P., Scalapino, D.J., Maiti, S., Hirschfeld, P.J., Adelmann, P., Wolf, T., Hai-Hu Wen, H.-H. and Rudi Hackl, R. (2018) Microscopic Origin of Cooper Pairing in the Iron-Based Superconductor $Ba_{1-x}K_xFe_2As_2$. *Nature Physics Journal: Quantum Materials*, **3**, Article No. 48.

[21] Hosono, H., Yamamoto, A., Hiramatsu, H. and Ma, Y. (2018) Recent Advances in Iron-Based Superconductors toward Applications.

[22] Sentef, M., Kemper, A.F., Moritz, B., Freericks, J.K., Shen, Z.-X. and Devereaux, T.P. (2013) Examining Electron-Boson Coupling Using Time-Resolved Spectroscopy. *Physical Review X*, **3**, Article ID: 041033. https://doi.org/10.1103/PhysRevX.3.041033

[23] Tortello, M., Daghero, D., Ummarino, G.A., Stepanov, V.A., Jiang, J., Weiss, J.D., Hellstrom, E.E. and Gonnelli, R.S. (2010) Multigap Superconductivity and Strong Electron-Boson Coupling in Fe-Based Superconductors: A Point-Contact Andreev-Reflection Study of $Ba(Fe_{1-x}Cox)_2As_2$ Single Crystals. arXiv:1009.1572v2.

[24] Ji, H.S., Lee, G. and Shim, J.H. (2011) Small Anisotropy in Iron-Based Supercon-

ductors Induced by Electron Correlation. *Physical Review B*, **84**, Article ID: 054542. https://doi.org/10.1103/PhysRevB.84.054542

[25] Llano, M., Sevcilla, F.J. and Tapia, S. (2012) Cooper Pairs as Bosons. *International Journal of Modern Physics B*, **20**, 2931-2939. https://doi.org/10.1142/S0217979206034947

[26] Mukubwa, A.W., Odhiambo, J.O. and Makokha, J.W. (2018) Thermodynamic Properties of Yttrium Based Cuprate Due to Electron-Cooper Pair Interaction Using BVT. *Open Access Library Journal*, **5**, e4880. https://doi.org/10.4236/oalib.1104880

[27] Cilento, F., Conte, D., Coslovich, D., Peli, S., Nembrini, N., Mor, S., Banfi, F., Ferrini, G., Eisaki, H., Chan, M.K., Dorow, C.J., Veit, M.J., Greven, M., Marel, D., Comin, R., Damscelli, A., Retig, L., Bovoenspien, U., Capona, M., Gianetti, C. and Parmigiani, F. (2014) Photo-Enhanced Antinodal Conductivity in the Pseudogap State of TC Cuprates. *Nature Communication*, **5**, Article No. 4353. https://doi.org/10.1038/ncomms5353

[28] Howald, L., Stilp, E., de Reotier, D.P., Yaouanc, A., Raymond, S., Piamonteze, C., Lapertot, G., Baines, C. and Keller, H. (2015) Evidence of Coexistence of Bulk Superconductivity and Itinerant Antiferromagnetism in the Heavy Fermion System $CeCo(In_{1-x}Cd_x)_5$. *Scientific Report*, **5**, Article No. 12528.

[29] Kibe, H.E., Sakwa, T.W. and Khanna, K.M. (2017) Specific Heat of the Integrated S-Wave and P-Wave Pairing in Uranium and Cerium Based Heavy Fermion Superconductors. *International Journal of Physics and Mathematical Sciences*, **7**, 1-6.

[30] Kim, J.S., Zhao, K., Jin, C.Q. and Stewart, G.R. (2014) Specific Heat of $Ca_{0.33}Na_{0.67}Fe_2As_2$. *Solid State Communications*, **193**, 34-36. https://doi.org/10.1016/j.ssc.2014.05.018

[31] Loram, J.W., Mirza, K.A., Cooper, J.R. and Liang, W.Y. (1993) Electronic Specific Heat of $YBa_2Ca_3Cu_3O_{6+x}$ from 1.8 to 300K. *Physics Review Letter*, **71**, 1740. https://doi.org/10.1103/PhysRevLett.71.1740